Electric field modulation of synchronization in neuronal networks

E.-H. Park[1,3], P. So[1,3], E. Barreto[1,3], B. J. Gluckman[1,3], and S. J. Schiff[2,3]
[1]Department of Physics & Astronomy, [2]Department of Psychology, and
[3]The Krasnow Institute for Advanced Study, Mail Stop 2A1
George Mason University, Fairfax, VA 22030 USA

Keywords: synchronization, electric field, seizures, hippocampus, CA1

Abstract

Motivated by the observation that applied electric fields modulate hippocampal seizures, and that seizures may be asynchronous, we modeled synaptically-coupled 2-compartment hippocampal pyramidal neurons embedded within an electrically resistive lattice in order to examine network synchronization properties under the influence of externally applied electric fields. Excitatory electric fields were shown to synchronize or desynchronize the network depending on the natural frequency mismatch between the neurons. Such frequency mismatch was found to decrease as a function of increasing electric field amplitude. These findings provide testable hypotheses for future seizure control experiments.

Since the 1950s, it been generally assumed that seizures are manifestations of excessive synchrony. However, recent experiments using dual intracellular impalements in the CA1 region of rat hippocampal slices suggest that neurons may *desynchronize* as seizures initiate, and resynchronize as seizures terminate. In addition, theoretical work has recently established that sustained activity can be supported by collectively *asynchronous* states [7]. These results, in juxtaposition with recent demonstrations that electric fields can modulate neuronal dynamics and suppress seizure-like activity [4,5], have motivated the present work. We seek to gain a better

understanding of the synchronization properties of populations of neurons, and in particular, how such synchrony may be modulated with electric fields.

We report results based on a computational model that we have explicitly designed to include electric field interactions. Since the presence of an electric field induces spatial polarization in neurons [1,2,12], the minimum individual neuronal unit must have at least two spatially separated compartments. We therefore chose the two-compartment lumped Pinsky-Rinzel (PR) model neuron, which consists of a dendritic and a somatic compartment separated by a finite conductance [10]. For the present work, two such neurons were embedded within a lattice of resistors which models the extracellular medium, and a potential difference was imposed along the somatic-dendritic axis. In addition to interacting electrically via the resistive network, the neurons were also coupled via AMPA and NMDA synapses.

A schematic representation of the PR model neuron is shown in Figure 1(a). Specific details can be found in [5,10][1]. Two neurons were arranged in the resistive array as shown in Figure 1 (b), and an externally applied electric field was introduced by imposing a potential difference between V_{app} and ground. In addition to varying V_{app}, we also vary the difference Δg_c between the neurons' internal soma-dendrite conductances ($g_c^{(1)} = 2.1\,\mathrm{mS/cm^2}$, and $g_c^{(2)} = (1-\delta)g_c^{(1)}$, where $\delta = 0-30\%$) .

To characterize synchronization, we employed a phase locking index γ defined by $\gamma^2 = \langle \cos\Psi(t) \rangle^2 + \langle \sin\Psi(t) \rangle^2$ [8,11], where <> denotes time-average. Ψ(t) is the relative phase, defined as $\Psi(t_k^{(1)}) = 2\pi \left(t_k^{(1)} - t_m^{(2)} \right) \Big/ \left(t_{m+1}^{(2)} - t_m^{(2)} \right)$, where m and n are event numbers for neurons 1 and 2,

[1] The parameters were chosen as in Ref. [10], with Id=0.7 μA/cm^2, Is=0, $g_{NMDA} = 0.03$ mS/cm^2 $g_{AMPA} = 0.0045$ mS/cm^2 and $[K^+]_o$=3.5 mM. The potassium reversal potential relative to –60 mV is V_K = -38.56 mV.

respectively, and the times t are defined by threshold crossings. Figure 2(a) shows sample tracings of the somatic voltages and illustrates

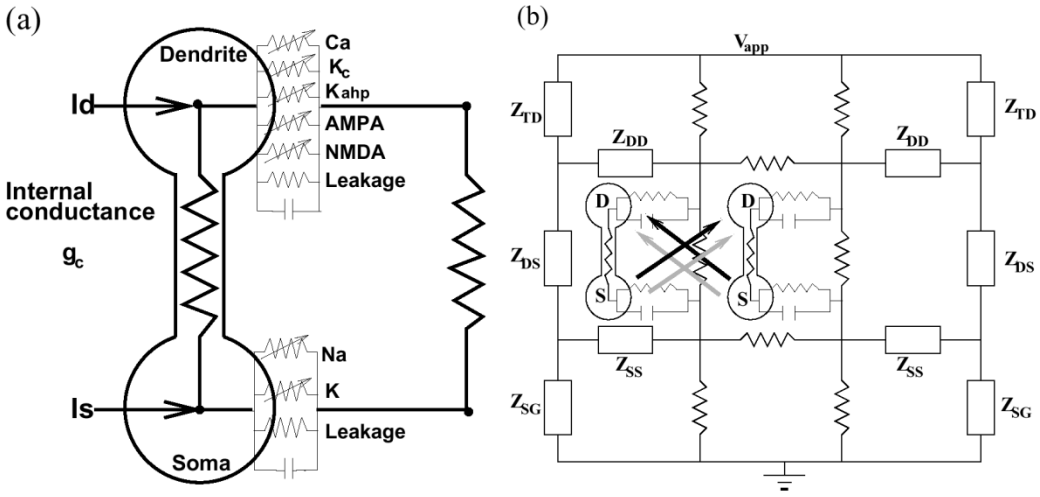

Figure 1: (a) Currents and conductances for a single PR neuron. (b) Synaptically coupled neurons embedded within a resistive array modeling the electric properties of CA1. Black and gray arrows indicate NMDA and AMPA excitatory synapses, respectively. The terminal resistances are chosen such that the lattice is equivalent to a horizontally-infinite lattice.

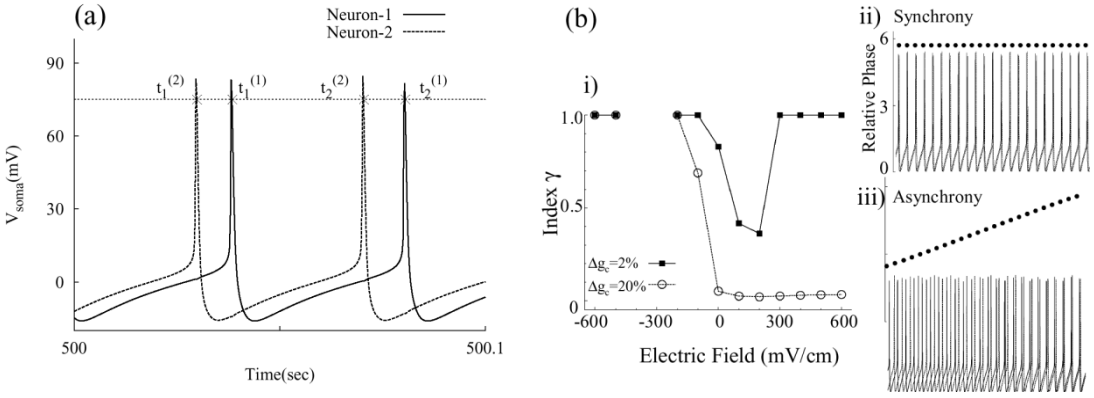

Figure 2: (a) Tracings of the somatic voltage from two neurons within the network. (b) i) γ vs. electric field strength for two different levels of parameter mismatch. γ and $V_{soma}^{(1,2)}$ as a function of time in ii) the synchronous case and iii) asynchronous case.

the procedure for calculating γ. Note that γ varies between 0 and 1 for unsynchronized and synchronized activity, respectively.

Figure 2(b) shows that by varying the strength of the applied electric field, the neurons either synchronize or desynchronize depending on the parameter mismatch Δg_c. Neurons with large parameter mismatch are observed to phase-lock for moderate inhibitory (negative) electric fields, and to desynchronize as the field becomes excitatory (positive). However, for small parameter mismatch, we observed that the neurons then resynchronize for sufficiently large excitatory fields. This is consistent with results reported by Golomb and Hansel [6], who found that in heterogeneous ensembles, increasing coupling tends to desynchronize the network.
A more complete summary of our network's dynamics is presented in Figure 3(a). Here, we show the γ index as a function of both the applied electric field strength and the parameter mismatch Δg_c. Several features are prominent. An extensive asynchronous region is present for large excitatory fields and large neuronal disparity, again, in agreement with Golomb and Hansel's observation in [6]. Second, large inhibitory fields tend to induce phase locking even when neuronal disparity is large. Third, moderate inhibitory fields suppress collective network activity (consistent with the *In Vitro* seizure suppression experiments of Gluckman et al. [4,5]). Perhaps the most interesting feature of this phase diagram is the boundary between the phase-locked and asynchronous states. As observed in Figure 2(b), for small neuronal disparity there is a regime where moderately strong excitatory fields desynchronize the network, but an even stronger field leads to resynchronization. This threshold is seen in Figure 3(a) to increase with increasing Δg_c.

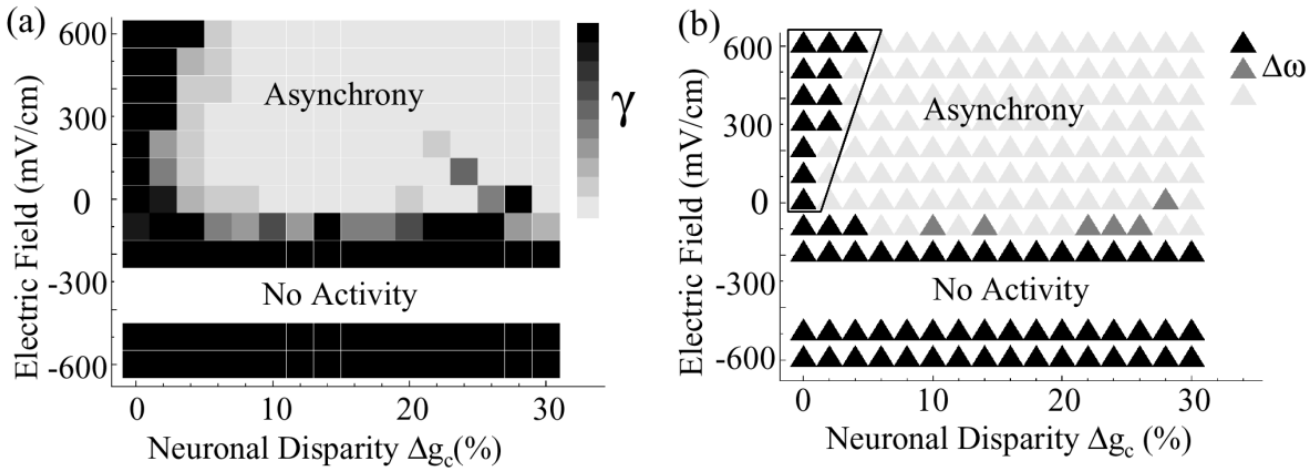

Figure 3: (a) Synchrony phase diagram. γ is plotted in gray-scale (black=1, white=0) as a function of the electric field strength and the neuronal disparity. Network activity is fully suppressed by moderate inhibitory applied fields of approximately –300 to –400 mV/cm. (b) Natural frequency mismatch $\Delta\omega$ between the neurons as a function of the applied electric field and neuronal disparity (dark triangle indicates $\Delta\omega$ <0.1; medium triangle indicates $\Delta\omega$~0.1; light gray triangle indicates $\Delta\omega$>0.1).

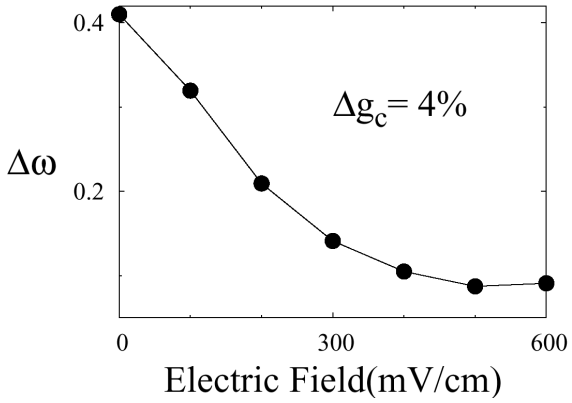

Figure 4: Natural frequency mismatch $\Delta\omega$ as a function of the applied electric field for $\Delta g_c = 4\%$.

We now argue that this nontrivial boundary can be explained using a simple phase oscillator model [3,8,13]. In our network, the dynamics of the individual units are predominately periodic spikes or bursts which are well approximated by a system of coupled phase oscillators for a significant range of parameters. Details pertaining to the reduction of our system will be presented elsewhere [9]. Here, we show that this simple approach explains the synchrony/asynchrony boundary described above.

Figure 3(b) shows the degree of natural frequency mismatch $\Delta\omega$ between our two individual units as a function of applied electric field and neuronal disparity. To measure $\Delta\omega$, each neuron was observed in isolation, subject only to the applied electric field. The boundary defined by $\Delta\omega = \alpha \simeq 0.1(Hz)$ is such that for $\Delta\omega > \alpha$, the network is in the asynchronous state, and for $\Delta\omega < \alpha$, the neurons phase lock to each other. It is remarkable that this simple criterion reproduces the observed transition boundary rather well. In particular, it correctly predicts that for small neuronal disparity ($\Delta g_c < 6\%$), increasing the (excitatory) electric field first desynchronizes and then resynchronizes the network (see the circled region in Figure 3(b)). To clarify this point, the inset shows that $\Delta\omega$ decreases for increasing (excitatory) electric field at $\Delta g_c = 4\%$. One can understand this by noting that each individual neuron's spiking rate is a concave-down function with respect to the applied electric field. Thus, as the spiking rate increases, the corresponding *incremental* increase is smaller. In the small disparity regime, the initial frequency mismatch is small enough such that as the excitatory field increases, the difference between the spiking rates of the two neurons decreases below the critical level $\Delta\omega^* = \alpha$, and phase locking is observed.

Conclusion

We have demonstrated that a computational model of two-compartment neurons embedded within a resistive extracellular medium exhibits both complex phase locking and asynchronous behavior as a function of the applied electric field and the degree of neuronal disparity. The observed dynamics are consistent with recent theoretical and experimental results. Most importantly, there exists a critical value of natural frequency mismatch which determines the synchronization properties of the network. We speculate that the observed phase-locking threshold may be explained in terms of a system of coupled phase oscillators.

This work was supported by NIH K02MH01493, 2R01MH50006, K25 MH01963; NSF IBN 97-27739

References

[1] C. Y. Chan and C. Nicholson, Modulation by applied electric fields of Purkinje and stellate cell activity in the isolated turtle cerebellum. J. Physiol. (Lond.) 371 (1986) 89-114.

[2] C. Y. Chan, J. Houndsgaard, and C. Nicholson, Effects of electric fields on transmembrane potential and excitability of turtle cerebellar Purkinje cells In Vitro. J. Physiol. (Lond.) 402 (1988) 751-771.

[3] A. H. Cohen, P. J. Holmes, and R. H. Rand, The nature of the coupling between segmental oscillators of the lamprey spinal generator for locomotion: a mathematical model. J. Math. Bio. 13 (1982) 345-369.

[4] B. J. Gluckman, H. Nguyen, S. L. Weinstein, and S. J. Schiff, Adaptive Electric Field suppression of Epileptic Seizures, Journal of Neuroscience 21 (2001) 590-600.

[5] B. J. Gluckman, P. So, T. I. Netoff, M. Spano, and S. J. Schiff, Stochastic Resonance in Mammalian Neuronal networks, Chaos 8 (1998) 588-598.

[6] D. Golomb and D. Hansel, The number of synaptic inputs and the synchrony of large, sparse neuronal networks. Neural Comp. 12 (2000) 1095-1139.

[7] B. S. Gutkin, C.R. Lang, C. L. Colby, C. C. Chow, and G. B. Ermentrout, Turning on and off with excitation: the role of spike-timing asynchrony and synchrony in sustained neural activity. Journal of Computational Neuroscience 11 (2001) 121-134.

[8] Y. Kuramoto, Chemical oscillations, waves, and turbulence (Springer, Berlin, 1984).

[9] E.-H. Park, P. So, E. Barreto, and S. J. Schiff, in preparation.

[10] P. F. Pinsky and J. Rinzel, Intrinsic and network rhythmogenesis in a reduced Traub model for CA3 neurons, J Comput Neurosci. 1 (1994) 39-60.

[11] A. Pikovsky, M. Rosenblum, and J. Kurths, Synchronization a universal concept in nonlinear sciences (Cambridge University Press, 2001).

[12] D. Tranchina and C. Nicholson, A model for the polarization of neurons by extrinsically applied electric fields. Biophys. J. 50 (1986) 1139-1159.

[13] A. T. Winfree, The geometry of biological time (Springer, New York, 1980).